



# The Water Cycle of the Baltic Sea Region From GRACE/GRACE-FO Missions and ERA5 Data

Ahmed Kamel Boulahia<sup>1</sup>, David García-García<sup>1\*</sup>, M. Isabel Vigo<sup>1</sup>, Mario Trottini<sup>2</sup> and Juan-Manuel Sayol<sup>1</sup>

<sup>1</sup>Applied Mathematics Department, University of Alicante, Alicante, Spain, <sup>2</sup>Mathematics Department, University of Alicante, Alicante, Spain

The water cycle of the Baltic Sea has been estimated from the Gravity Recovery and Climate Experiment (GRACE) and the GRACE Follow-On satellite time-variable gravity measurements, and precipitation and evaporation from ERA5 atmospheric reanalysis data for the periods 06/2002 to 06/2017 and 06/2018 to 11/2021. On average, the Baltic Sea evaporates  $199 \pm 3 \text{ km}^3/\text{year}$ , which is overcompensated with  $256 \pm 6 \text{ km}^3/\text{year}$  of precipitation and  $476 \pm 17 \text{ km}^3/\text{year}$  of water from land. This surplus of freshwater inflow produces a salty water net outflow from the Baltic Sea of  $515 \pm 27 \text{ km}^3/\text{year}$ , which increases to  $668 \pm 32 \text{ km}^3/\text{year}$  when the Kattegat and Skagerrak straits are included. In general, the balance among the fluxes is not reached instantaneously, and all of them present seasonal variability. The Baltic net outflow reaches an annual minimum of  $221 \pm 79 \text{ km}^3/\text{year}$  in September and a maximum of  $814 \pm 94 \text{ km}^3/\text{year}$  in May, mainly driven by the freshwater contribution from land. On the interannual scale, the annual mean of the Baltic net outflow can vary up to  $470 \text{ km}^3/\text{year}$  from year to year. This variability is not directly related to the North Atlantic Oscillation during wintertime, although the latter is well correlated with net precipitation in both continental drainage basins and the Baltic Sea.

## OPEN ACCESS

### Edited by:

Mehdi Eshagh,  
University West, Sweden

### Reviewed by:

Farzam Fatolazadeh,  
Université de Sherbrooke, Canada  
Andenet Gedamu,  
Addis Ababa University, Ethiopia

### \*Correspondence:

David García-García  
d.garcia@ua.es

### Specialty section:

This article was submitted to  
Solid Earth Geophysics,  
a section of the journal  
Frontiers in Earth Science

**Received:** 18 February 2022

**Accepted:** 06 April 2022

**Published:** 12 May 2022

### Citation:

Boulahia AK, García-García D, Vigo MI,  
Trottini M and Sayol J-M (2022) The  
Water Cycle of the Baltic Sea Region  
From GRACE/GRACE-FO Missions  
and ERA5 Data.  
Front. Earth Sci. 10:879148.  
doi: 10.3389/feart.2022.879148

**Keywords:** Baltic Sea, water cycle, water transport, runoff, Skagerrak–Kattegat, Danish straits

## INTRODUCTION

The hydrological or water cycle refers to the continuous movement of water in the atmosphere, continents, oceans, and among them. It regulates the weather and determines the availability of fresh water, which is vital for both human and ecosystem life. Understanding the water cycle of a region is crucial to manage freshwater resources and then human and natural life. As the hydrological cycle is both cause and consequence of the climate of any region, it is vulnerable to climate change. At present, the global hydrological cycle is intensifying (Durack et al., 2012; Markonis et al., 2019), which is unsurprising under the ongoing global warming scenario (Held and Soden, 2006; Huntington, 2006; Greve et al., 2014). In addition, the monitoring of water cycles and their time evolution should be done at a regional scale since the response of each region to changes in the hydrological cycle is different. Giorgi (2006) estimated the vulnerability of several regions based on results from a multi-model ensemble of climate change simulations. The most vulnerable regions are the Mediterranean and northeastern Europe regions. The second most vulnerable regions are a tropical region (Central America) and three regions with high latitude cold climate (northern Europe, Greenland, and Northern Asia). Here, we study the hydrological cycle of the Baltic Sea, in

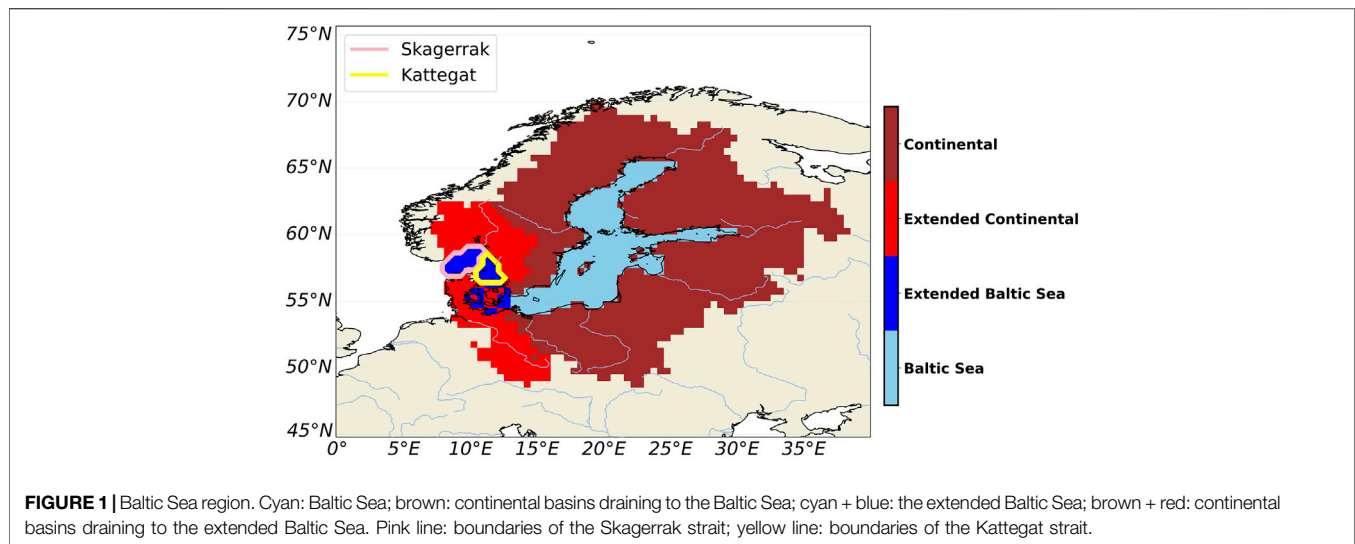


**TABLE 1** | Reported values of runoff into the Baltic Sea from the literature and estimated  $R$  in the present study. Units are  $\text{km}^3/\text{year}$ . Acronyms: REMO, Regional Model; ECMWF, European Centre for Medium-Range Weather Forecasts; ECHAM, European Centre Hamburg Model; RCO, Rossby Centre Ocean Model; RCAO, Rossby Centre Atmosphere–Ocean Model; BALTEX, Baltic Sea Experiment; BACC, BALTEX Assessment of Climate Change for the Baltic Sea Basin.

	Specification	Period	Baltic Sea
Mikulski (1986)	Historical data (the Belt Sea and Kattegat excluded)	1951–1970	436
	(The Belt Sea and Kattegat included)	1951–1970	473
Bergstrom and Carlsson (1994)	<i>In situ</i>	1950–1990	483
Matthäus and Schinke (1999)	Historical data	1899–1993	428
Cyberski and Wróblewski (2000)	Historical data	1901–1990	480
Omstedt and Rutgersson (2000)	Historical data	1980–1995	478
Jacob (2001)	REMO with ECMWF re-analyses	1981–1988	439
	REMO is driven by ECHAM4/T106 data	1979–1988	522
	ECHAM4/T106	1979–1988	497
Winsor et al. (2001)	Historical data	1920–1990	442
	Same but including the Kattegat + Danish straits		479
Meier and Döscher (2002)	RCO	1980–1993	475
	RCO	1988–1993	465
	RCAO	1988–1993	507
Lehmann and Hinrichsen (2002)	Historical data	1979–1990	520
Meier and Kauker (2003)	Historical data	1902–1998	444
Omstedt et al. (2004)	Historical data	1993–2002	442
The BACC Author Team (2008)	BALTEX programme	1921–1998	445
Hansson et al. (2011)	Statistical model	1,500–1995	486 ± 28
Hänninen and Vuorinen (2011)	Historical data. The 12 largest rivers	1970–2000	263
Johansson (2016)	Historical and modeled data	1950–2013	499
Literature summary (excluding Hänninen and Vuorinen, 2011)	Mean ± SD of these values (excluding this study)	—	473 ± 12
This study: the Baltic Sea	GRACE and ERA5 atmospheric model	06/2002–06/2017 and 06/2018–11/2021	476 ± 17
Extended Baltic Sea			618 ± 21

northern Europe, following the same approach of a previous study focused on the Mediterranean-Black Sea system (García-García et al., 2022).

The Baltic Sea is an intracontinental and semi-enclosed basin of  $\sim 380 \cdot 10^3 \text{ km}^2$  surrounded by nine countries: Denmark, Germany, Poland, Lithuania, Latvia, Estonia, Russia, Finland, and Sweden. It is a shallow sea with 55 m of average depth and 459 m of maximum depth (Daraghi et al., 2017). The continental drainage region is inhabited by  $\sim 85$  million people, whose

livelihood largely depends on the sea. The Baltic Sea is connected to the North Atlantic Ocean at the North Sea through three consecutive straits. From the Baltic Sea to the North Sea, we find the following: 1) the Danish straits, which consist of three small straits: the Great Belt (60 km long and 16–32 km wide), the Little Belt (50 km long and 0.8–28 km wide), and the Øresund (118 km long and 4–28 km wide); 2) the Kattegat Strait (220 km long and 60–142 km wide); and 3) Skagerrak Strait (240 km long and 130–145 km wide)

**TABLE 2** | Reported values of net seawater outflow from the Baltic Sea from the literature and the present study. Outflow means WT leaving the Baltic Sea. The extended Baltic Sea includes the Kattegat and Skagerrak straits. Units are km<sup>3</sup>/year. Acronyms: PROBE, Program for Boundary Layers in the Environment; CoastMab, a process-based mass-balance model for phosphorus for coastal areas; RCO-A, assimilation/reanalysis setup of the RCO model.

	Specification	Location of the net outflow	Period	Net outflow	Inflow	Outflow
Mikulski (1986)	Based on sea level monitoring with adjustment	Danish straits (without the Belt Sea)	1951–1970	471	—	—
		Danish straits (with the Belt Sea)	1951–1970	485	—	—
Omstedt and Rutgersson (2000)	PROBE-Baltic ocean model	Kattegat through Danish straits	1980–1995	534	1,290	1825
Jacob (2001)	ECHAM4/T106	Kattegat through	1979–1988	606	—	—
	REMO is driven by ECHAM4/T106 data	Danish straits	1979–1988	621	—	—
	REMO with ECMWF re-analyses		1981–1988	517	—	—
Winsor et al. (2001)	Using sea level data from Hornbaek	Danish straits	1921–1990	473	2050	2,523
Lehmann and Hinrichsen (2002)	Based on the Bryan–Cox–Semtner general circulation model with a free surface	Arkona Basin	1979–1990	513	—	—
Omstedt and Nohr (2004)	PROBE-Baltic ocean model	Danish straits (without the Belt Sea)	1979–2002	529	1,348	1874
			2000–2002	564	1,212	1776
Hakanson and Lindgren (2010)	Mass balance, CoastMab model	Kattegat through Danish straits	1997–2005	540	345	885
Dargahi and Cvetkovic (2017)	Numerical simulations of the hydrodynamics that are verified by salinity and temperature data	Danish straits	2000–2009	311	1,563	1874
Placke et al. (2018)	RCO-A	Arkona Basin	1970–1999	442	—	—
Literature summary	Mean ± SD of these values (excluding this study)	—	—	508 ± 22	1,301 ± 227	1793 ± 214
This study: the Baltic Sea	GRACE and ERA5 atmospheric model	Longitude 13°E (Arkona Sea)	06/2002–06/2017 and 06/2018–11/2021	515 ± 27	—	—
Extended Baltic Sea	Indirect estimate of <i>R</i>	Longitude 8°E		668 ± 32	—	—

(Figure 1). Vertically, the Baltic Sea exchanges fresh water with the atmosphere *via* precipitation (*P*) and evaporation (*E*). Horizontally, the Baltic Sea receives fresh water from the surrounding lands (*R*), where the excess of *P* over *E* that is not stored on land must flow to the sea. Then, *R* accounts for river runoff, but also for surface runoff outside the course of the rivers and submarine groundwater discharge to the ocean. River runoff for this region has been previously estimated, from *in situ* observations and models, with values between 428 and 522 km<sup>3</sup>/year from different methodologies, data sets, and periods of time (see Table 1). Also horizontally, the Baltic Sea exchanges salty water with the North Sea in a way that can be approximated by a two-layer model: at the bottom layer, the North Sea introduces saltier (and denser) water into the Baltic Sea, while at the top one, fresher (and less dense) water flows in the opposite sense (e.g., The BACC Author Team, 2008; Hanninen et al., 2021). Outflow is lighter than inflow because *P* and *R* exceed *E* in the Baltic Sea freshening the water. The imbalance between the inflow and the outflow results in a net outflow leaving the Baltic Sea, denoted by *N*, that oscillates between 311 and 621 km<sup>3</sup>/year, as estimated from current and sea level observations, and numerical models (see Table 2). This situation opposes the one found in another semi-enclosed sea, the Mediterranean Sea, where *E* exceeds *P* and *R*, and highly saline water sinks to the bottom and then is transported to the North Atlantic Ocean through the Strait of Gibraltar, while less salty water flows near the surface in the opposite sense (Jordà et al., 2017, and references therein). The exchange of salty water

together with other biogeochemical tracers is important, for example, for the organisms living in the deep waters of the Baltic Sea, which rely on the inflows of extremely salty and oxygenated water from the North Sea (Stramska and Aniskiewicz, 2019).

In 2002, the GRACE (Gravity Recovery and Climate Experiment) satellite mission was launched to estimate time-variable gravity data, which is corrected for some known geophysical signals as, for example, solid and ocean tides, pole tides, or gravitational perturbations from the Sun, Moon, and solar system planets. Assuming that the remaining gravity variations are produced by mass variations on the surface of the Earth (such as the water mass transport within the water cycle, the biggest mass variations of the Earth in the intra-annual timescale), the surface mass variation can be uniquely determined (Wahr et al., 1998; Chao, 2005). These data revolutionized the way to study the Earth (see Wouters et al., 2014, and references therein) since it produced a unique tool to understand the water mass transport in the Earth system, and hence the water cycle. In the Baltic region, GRACE data have been used to estimate the variability of the seawater budget, which explained more than half of the sea-level variations (Virtanen et al., 2010), and that of the terrestrial water budget in some coastal points (Pajak and Birylo, 2017). The main contribution of this study is a novel application of the GRACE data to estimate the net seawater mass exchange in the Baltic Sea using the algorithm proposed by García-García et al. (2020) that uses GRACE data to estimate the net water mass transport (WT)

among ocean basins and that allows to track the oceanic components of the water cycle. When the algorithm is applied to semi-enclosed basins, it is possible to estimate the water mass exchange between the basin and the open ocean as shown for the Mediterranean Sea by García-García et al. (2022). An additional contribution is the use of GRACE data to estimate the water discharge from the continents in the Baltic Sea, which mainly is runoff. For this second objective, we followed the same methodology used for related problems in other regions. For example, independent of *in situ* observations, GRACE data have been used to estimate runoff of major river basins such as the Amazon (Syed et al., 2005; Eom et al., 2017), Paraná (Lee et al., 2018), Mississippi (Syed et al., 2005), Yellow River (Li et al., 2016), and smaller river basins (Lorenz et al., 2014). Due to the global nature of GRACE measurements, GRACE data have also been used to estimate the  $R$  of whole continents and the  $R$  received for whole ocean basins (Syed et al., 2009).

For the net seawater mass exchange in the Baltic Sea, we have used time-variable gravity measurements from GRACE and GRACE Follow-On satellites (GRACE FO), as well as  $P$  and  $E$ , obtained from ERA5 atmospheric reanalysis data, to estimate the mean values and time-variable evolution of all the WT components involved in the water cycle of the Baltic Sea for the periods 06/2002 to 06/2017 and 06/2018 to 11/2021. GRACE and GRACE FO data are crucial to estimate  $R$  and  $N$  independently of *in situ* observations or models. The study is structured as follows: in the *Methods* and *Data* section, satellite-based gravimetric and reanalysis data used to study the hydrological cycle are described in detail, together with those methods applied to evaluate seasonal and nonseasonal signals of WT components, and their uncertainties; *Results* section shows the main results found for all WT terms, including the time mean, the seasonal cycle, and the nonseasonal signal, as well as their connection with the North Atlantic Oscillation; finally, in the *Discussion* and *Conclusion* sections the main results are discussed and outlined, respectively.

## METHODS AND DATA

This section describes the following: 1) the methodology used to estimate  $R$  and  $N$  in the Baltic Sea, as well as the theoretical frame to estimate the associated errors; 2) the data used, consisting of time-variable gravity, and  $P$  and  $E$  atmospheric variables from a reanalysis atmospheric model, as well as the applied corrections.

### Methods

The estimation of  $P$ ,  $E$ ,  $R$ , and  $N$ , as well as their time evolution, is key to understanding the regional water cycle. In the Baltic Sea, all WT components are related *via* the water balance equation:

$$dW = P - E + R + N, \quad (1)$$

where the new term  $dW$  represents the change in water content in the region. According to the equation, positive (negative) values of  $N$  represent inflows to (outflows from) the Baltic Sea. If  $P$ ,  $E$ , and  $dW$  are known, then  $R$  and  $N$  can be estimated in a two-step

process (García-García et al., 2020; 2022). First, **Eq. 1** is applied to the continental catchment region draining to the Baltic Sea, which is identified according to the global continental runoff pathway scheme (Oki and Sud, 1998). Note that in this case  $N = 0$  and  $R$  is estimated as a residual. Second, **Eq. 1** is applied to the Baltic Sea and  $N$  is estimated as a residual.

For each WT time series, the following harmonic regression model with linear trend, and annual and semiannual components has been considered (e.g., Jin and Feng, 2013; Fatolazadeh and Goïta, 2021):

$$C_t = p_0 + p_1 \cdot t + A_a \cos(\omega_a \cdot t - \phi_a) + A_{sa} \cos(\omega_{sa} \cdot t - \phi_{sa}), \quad (2)$$

where  $t$  represents time,  $C_t$  is the value of the time series of interest at time  $t$ ,  $(\omega, A, \phi) = (\text{frequency, amplitude, phase})$ , and the suffixes  $a$  and  $sa$  denote annual and semiannual terms, respectively. Note that  $\phi_a$  determines when the annual maximum is reached, since a degree is roughly equivalent to a day of the year. Using the angle subtraction cosine formula, the model in **Eq. 2** can be written as a linear regression model with independent variables:  $\cos(\omega_a \cdot t)$ ,  $\sin(\omega_a \cdot t)$ ,  $\cos(\omega_{sa} \cdot t)$ , and  $\sin(\omega_{sa} \cdot t)$ . Then, **Eq. 2** can be rewritten as

$$C_t = p_0 + p_1 \cdot t + a_1 \cos(\omega_a \cdot t) + b_1 \sin(\omega_a \cdot t) + a_2 \cos(\omega_{sa} \cdot t) + b_2 \sin(\omega_{sa} \cdot t), \quad (3)$$

where

$$a_1 = A_a \cos(\phi_a), b_1 = A_a \sin(\phi_a), \quad (4)$$

$$a_2 = A_{sa} \cos(\phi_{sa}), b_2 = A_{sa} \sin(\phi_{sa}). \quad (5)$$

The parameters  $p_0$ ,  $p_1$ ,  $a_1$ ,  $b_1$ ,  $a_2$ , and  $b_2$  in **Eq. 3** are estimated by ordinary least squares. Then,  $(A_a, \phi_a)$  and  $(A_{sa}, \phi_{sa})$  are estimated from **Eqs 4, 5**, respectively. In particular, we have

$$A_a = \sqrt{a_1^2 + b_1^2}, \quad A_{sa} = \sqrt{a_2^2 + b_2^2}.$$

The annual component is considered not statistically significant when the  $p$ -value for both coefficients  $a_1$  and  $b_1$  in the linear regression in **Eq. 3** is greater or equal to 0.05. The same reasoning is used to assess the statistical significance of the semiannual component.

The reported standard deviations (SD) and 95% confidence intervals (CI) for the averages, trends, and seasonal signals of the components of the WT, as well as for correlations, have been evaluated using the stationary bootstrap scheme of Politis and Romano (1994) with the optimal block length selected according to Patton et al. (2009) as well as the percentile method. Note that each time series comprises 221 observations and can be seen as the junction of two evenly spaced time series (with 181 observations from June 2002 to June 2017, and 40 observations from June 2018 to November 2021) separated by a gap of 11 months. Since the stationary bootstrap assumes evenly spaced data, the distributions and the SD of the estimators of the quantities of interest were obtained by applying the bootstrap to the first series (of length 181). In all cases, the distribution of the

estimator was approximately normal; thus, the corresponding 95% CI can be obtained as the mean of the bootstrap estimates plus/minus 2 SD. In order to make full use of the data, in the calculation of 95% CI, averages of the bootstrap estimates based on the reduced series (with 181 observations) were replaced by the estimate of the quantity of interest based on the original time series (with 221 observations). To simplify the notation, all results in this study are provided in the form estimate  $\pm$ SD. The implementation of the stationary bootstrap used here is very similar to the one used in the study by García-García et al. (2020) and García-García et al. (2022), and further details can be found there. The number of bootstrap replications was set to 10,000.

As a sensitivity check, the analysis was repeated including a third cosine term in Eq. 2 to account for the 161-day signal due to the S2 aliasing in the GRACE data. The results of the analysis with and without this additional cosine term were identical.

## Data

Net precipitation,  $P-E$ , is obtained from the ERA5 reanalysis (Hersbach et al., 2018; data accessed on 26/01/2022), which incorporates observational data into general-circulation modeling supplied by the European Centre for Medium-Range Weather Forecasts (ECMWF). It provides monthly (and hourly) coverage of all continents and seas. As data are available in a  $0.25^\circ$  regular grid for 2002–2021, they have been resampled to a  $0.5^\circ$  regular grid by simple averaging to match the spatial resolution of the continental drainage basin data.

Water mass budget variations,  $dW$ , are estimated from the RL06 GRACE mascon (mass concentration) v2 solution provided by the Center of Space Research (CSR) at the University of Texas at Austin (Save et al., 2016; Save, 2019; data accessed on 26/01/2022) for the period of May 2002–November 2021. Time series have missing values between the end of the GRACE mission and the beginning of the GRACE FO, that is, from July 2017 to May 2018. Moreover, the values of 12 single months and 5 pairs of consecutive months were missing and have been linearly interpolated. Data are on a  $0.25^\circ$  regular grid, but we have re-gridded them to  $0.5^\circ$  regular grids as we did for  $P-E$ . Note that the obtained spatial resolution is still finer than the  $\sim 300$  km ( $\sim 3^\circ$  near the Equator) resolution of GRACE, which measures gravity anomalies from month to month with respect to a dynamic geophysical model that accounts for solid and ocean tides, among other factors. Assuming that the gravity changes are produced by mass changes on the Earth's surface, such as in the oceans, the mascon solution can be interpreted as water mass ( $W$ ) budget anomalies (Chao, 2016). Time variations of  $W$  (that is,  $dW$ ) are estimated as the discrete central derivative of  $W$ ,

$$dW(t) = \frac{dW(t+1) - dW(t-1)}{2},$$

where  $t$  refers to any given month. As a result,  $dW$  data span from June 2002 to June 2017 and from June 2018 to November 2021. The same months are selected for  $P-E$  data.

In the mascon solution, the following usual corrections are applied by CSR to time-variable data, which include measurements from both GRACE and GRACE FO missions: 1) a solution from Satellite Laser Ranging was used to replace the  $C_{20}$  coefficient (Cheng and Ries, 2017); 2)  $C_{30}$  coefficient is also replaced,

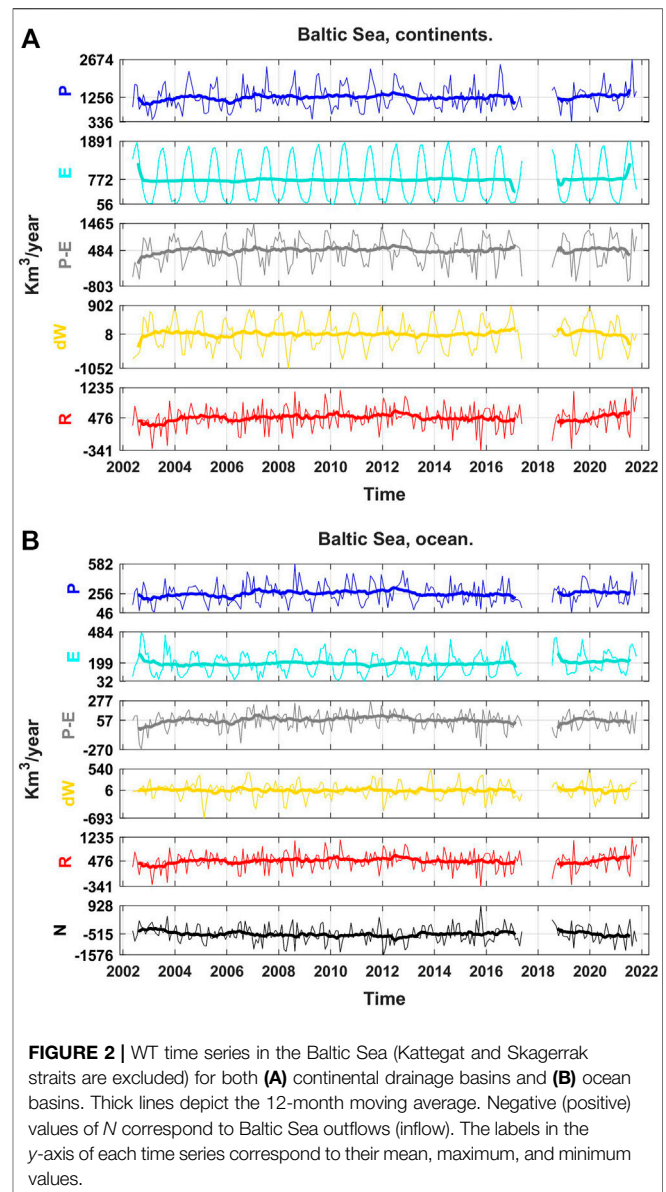


**FIGURE 2** | WT time series in the Baltic Sea (Kattegat and Skagerrak straits are excluded) for both (A) continental drainage basins and (B) ocean basins. Thick lines depict the 12-month moving average. Negative (positive) values of  $N$  correspond to Baltic Sea outflows (inflow). The labels in the y-axis of each time series correspond to their mean, maximum, and minimum values.

but only in data from the GRACE FO; 3) an estimate of the degree-1 coefficients was added (Swenson et al., 2008; Sun et al., 2016); 4) a glacial isostatic adjustment correction (GIA) was performed (Peltier et al., 2018). Moreover, we applied the following corrections: 5) the bottom pressure product (GAD), which accounts for nontidal fluctuations in both the atmosphere and the ocean, was added back to GRACE data with the mean value of the ocean set to zero to avoid inconsistencies with the following correction; 6) the degree-0,  $\Delta C_{00}$ , that accounts for changes in the total mass of the Earth. When the atmosphere is accounted for, there is no mass variation, and  $\Delta C_{00} = 0$ . However, when the atmosphere is excluded, the global mass of the Earth changes due to an exchange of water between the surface and the atmosphere. This mass exchange is not observed in GRACE since degree-0 coefficients are set to zero when atmospheric and dynamic oceanic mass changes are removed during the processing executed prior to data publication. To restore this

**TABLE 3** | Mean, annual, and semiannual signal, estimated from Eq. 2, for WT components for both the Baltic Sea and the extended Baltic Sea (Kattegat and Skagerrak straits are included) shown in Figure 2 and Supplementary Figure S1. Time spans from 06/2002–06/2017 to 06/2018–11/2021. Units are km<sup>3</sup>/year for mean values and amplitudes, and degrees for phases. In each cell the following are reported: 1) the point estimate (based on the original time series) plus/minus the standard deviation (SD; estimated by bootstrap based on the reduced series, that is from 181 observations); 2) the 95% confidence interval, CI, computed as the point estimate plus/minus 2 SD. Empty cells correspond to the amplitude of a phase of periodic (annual/semiannual) components not statistically significant at the significance level  $\alpha = 0.05$ . Regional surface areas are estimated with our grid resolution (see Figure 1). Negative *N* means a flux from the Baltic Sea to the North Sea. For the conversion of mass transport to volume transport, water density is fixed to 1,000 kg/m<sup>3</sup> for fresh water and 1,025 kg/m<sup>3</sup> for seawater.

		Mean $\pm$ SD, km <sup>3</sup> /year (95%CI)	Annual amplitude $\pm$ SD, km <sup>3</sup> /year (95% CI)	Annual phase $\pm$ SD, degrees (95% CI)	Semiannual amplitude $\pm$ SD, km <sup>3</sup> /year (95% CI)	Semiannual phase $\pm$ SD, degrees (95% CI)	Annual peak
Baltic Sea drainage basins (1.64 · 10 <sup>6</sup> km <sup>2</sup> )	<i>P</i>	1,256 $\pm$ 21 (1215, 1297)	395 $\pm$ 29 (338, 452)	215 $\pm$ 4 (207, 223)	196 $\pm$ 29 (137, 255)	7 $\pm$ 8 (–9, 23)	6 Aug
	<i>E</i>	772 $\pm$ 4 (764, 781)	839 $\pm$ 6 (826, 851)	183 $\pm$ 0.4 (182, 184)	187 $\pm$ 6 (175, 199)	2 $\pm$ 2 (–2, 6)	5 Jul
	<i>P–E</i>	484 $\pm$ 20 (444, 523)	547 $\pm$ 26 (495, 600)	340 $\pm$ 3 (335, 346)	—	—	11 Dec
	<i>dW</i>	8 $\pm$ 13 (–19, 35)	535 $\pm$ 21 (493, 577)	339 $\pm$ 2 (334, 344)	59 $\pm$ 22 (14, 104)	64 $\pm$ 39 (–14, 142)	10 Dec
	<i>R</i>	476 $\pm$ 17 (442, 510)	—	—	—	—	—
Baltic Sea (0.38 · 10 <sup>6</sup> km <sup>2</sup> )	<i>P</i>	256 $\pm$ 6 (244, 268)	93 $\pm$ 8 (77, 109)	277 $\pm$ 5 (267, 287)	23 $\pm$ 8 (7, 39)	5 $\pm$ 18 (–30, 40)	8 Oct
	<i>E</i>	199 $\pm$ 3 (193, 205)	119 $\pm$ 5 (110, 128)	272 $\pm$ 2 (267, 276)	27 $\pm$ 5 (18, 36)	90 $\pm$ 11 (68, 113)	3 Oct
	<i>P–E</i>	57 $\pm$ 7 (44, 70)	27 $\pm$ 9 (10, 45)	74 $\pm$ 21 (31, 117)	34 $\pm$ 9 (16, 52)	132 $\pm$ 17 (99, 165)	16 Mar
	<i>dW</i>	6 $\pm$ 4 (–2, 14)	151 $\pm$ 13 (125, 177)	260 $\pm$ 5 (250, 270)	—	—	21 Sep
	<i>N</i>	–515 $\pm$ 27 (–567, –463)	189 $\pm$ 39 (113, 265)	255 $\pm$ 11 (233, 278)	—	—	16 Sep
Extended Baltic Sea drainage basins (2.01 · 10 <sup>6</sup> km <sup>2</sup> )	<i>P</i>	1,584 $\pm$ 24 (1535, 1633)	475 $\pm$ 35 (405, 545)	217 $\pm$ 4 (209, 224)	249 $\pm$ 36 (176, 321)	7 $\pm$ 8 (–9, 23)	8 Aug
	<i>E</i>	956 $\pm$ 5 (946, 955)	1,015 $\pm$ 7 (1000, 1029)	183 $\pm$ 0.4 (182, 184)	217 $\pm$ 7 (203, 231)	2 $\pm$ 2 (–2, 5)	5 Jul
	<i>P–E</i>	628 $\pm$ 23 (583, 673)	673 $\pm$ 31 (610, 736)	340 $\pm$ 3 (334, 345)	—	—	11 Dec
	<i>dW</i>	10 $\pm$ 14 (–19, 38)	634 $\pm$ 23 (587, 680)	339 $\pm$ 2 (335, 343)	96 $\pm$ 29 (38, 154)	57 $\pm$ 24 (9, 106)	10 Dec
	<i>R</i>	618 $\pm$ 21 (576, 660)	—	—	—	—	—
Extended Baltic Sea (0.45 · 10 <sup>6</sup> km <sup>2</sup> )	<i>P</i>	319 $\pm$ 7 (305, 332)	112 $\pm$ 10 (92, 131)	277 $\pm$ 5 (267, 287)	29 $\pm$ 10 (9, 49)	1 $\pm$ 18 (–34, 35)	8 Oct
	<i>E</i>	245 $\pm$ 4 (239, 252)	138 $\pm$ 5 (128, 148)	266 $\pm$ 2 (262, 271)	27 $\pm$ 5 (17, 37)	86 $\pm$ 13 (61, 111)	27 Sep
	<i>P–E</i>	73 $\pm$ 8 (57, 89)	35 $\pm$ 11 (14, 56)	51 $\pm$ 24 (2, 99)	38 $\pm$ 11 (17, 60)	135 $\pm$ 18 (99, 170)	21 Feb
	<i>dW</i>	7 $\pm$ 5 (–2, 16)	165 $\pm$ 15 (137, 194)	262 $\pm$ 5 (252, 272)	—	—	23 Sep
	<i>N</i>	–668 $\pm$ 32 (–730, –606)	205 $\pm$ 45 (116, 293)	245 $\pm$ 13 (221, 270)	—	—	5 Sep

signal, we add the  $\Delta C_{00}$  term from ERA5 *P–E* to *dW* (Chen et al., 2019; García-García et al., 2020; 2022). Errors in the estimate of the  $\Delta C_{00}$  term propagate to the values of *dW*, but they do not affect the estimates of *R* and *N* from Eq. 1, since the  $\Delta C_{00}$  term vanishes due to the residual estimate between *dW* and *P–E*. In fact, adding  $\Delta C_{00}$  from *P–E* to GRACE is numerically equivalent to setting  $\Delta C_{00}$  of *P–E* to zero as far as Eq. 1 is concerned.

Volume transport is obtained from *P–E* by multiplying it (mm/month) with the surface of a cell grid in m<sup>2</sup> unit. On the other hand, the GRACE units are kg/m<sup>2</sup> for *W* and (kg/m<sup>2</sup>)/month for *dW*. Hence, *dW* provides mass transport when it is multiplied by the surface of a cell grid in m<sup>2</sup>. To compare *dW* and *P–E*, *dW* units are converted to volume transport units assuming a water density of 1,000 kg/m<sup>3</sup> for fresh water and 1,025 kg/m<sup>3</sup> for ocean water. In what follows, all results will represent volume transport and will be given in km<sup>3</sup>/year.

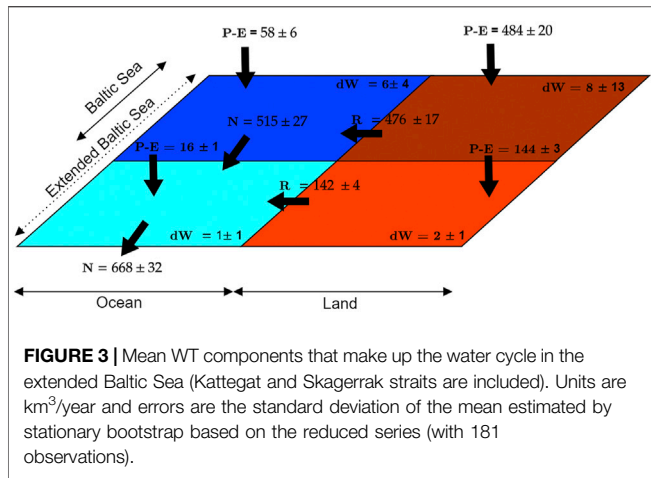
## RESULTS

We will consider two regions for the study of the hydrological cycle: 1) the Baltic Sea, with its western boundary defined by longitude 13° E in the Arkona Sea, and 2) the extended Baltic Sea, which includes the Kattegat and Skagerrak straits (Figure 1). We will show all results for 1), while those for 2) will be available as Supplementary Material. These results will be discussed in the context of previously published studies. The mean estimates of

each WT component in Eq. 1 for both continental drainage and oceanic basins of the Baltic Sea are shown in Figure 2 (those for the extended Baltic Sea are shown in the Supplementary Figure S1). Additionally, the seasonal and nonseasonal signals of the WT components are studied. Finally, the influence of the North Atlantic Oscillation (NAO) is also explored.

### Mean Values of WT

The mean values of all WT components of the Baltic Sea are shown in Table 3. The continental drainage basins receive net precipitation of 484  $\pm$  20 km<sup>3</sup>/year, which produces *R* = 476  $\pm$  17 km<sup>3</sup>/year (Table 1). This estimate of *R* agrees with the average of reported values of river runoff (Table 1). *P* also exceeds *E* in the sea, producing a net inflow of *P–E* = 57  $\pm$  7 km<sup>3</sup>/year, in contrast with the global ocean or the Mediterranean-Black Sea system where *E* exceeds *P* (Hartmann, 1994; García-García et al., 2020; García-García et al., 2022). Then, the excess fresh water given by *P–E* + *R* leaves the Baltic Sea through the Arkona Sea at a mean rate of 515  $\pm$  27 km<sup>3</sup>/year. Surprisingly, this value is identical, within error estimates, to the average net outflow, 508  $\pm$  23 km<sup>3</sup>/year, estimated from previously reported values (Table 2), despite the differences in the targeted period of study, methodology, and data used. The net WT component *N* is the result of a stratified water exchange in both senses. Saltier water from the Atlantic Ocean enters the Baltic Sea near the bottom at a mean rate of 1,301  $\pm$  227 km<sup>3</sup>/year, while less salty water leaves the Baltic Sea near the surface at a mean rate of 1,793  $\pm$  214 km<sup>3</sup>/year.

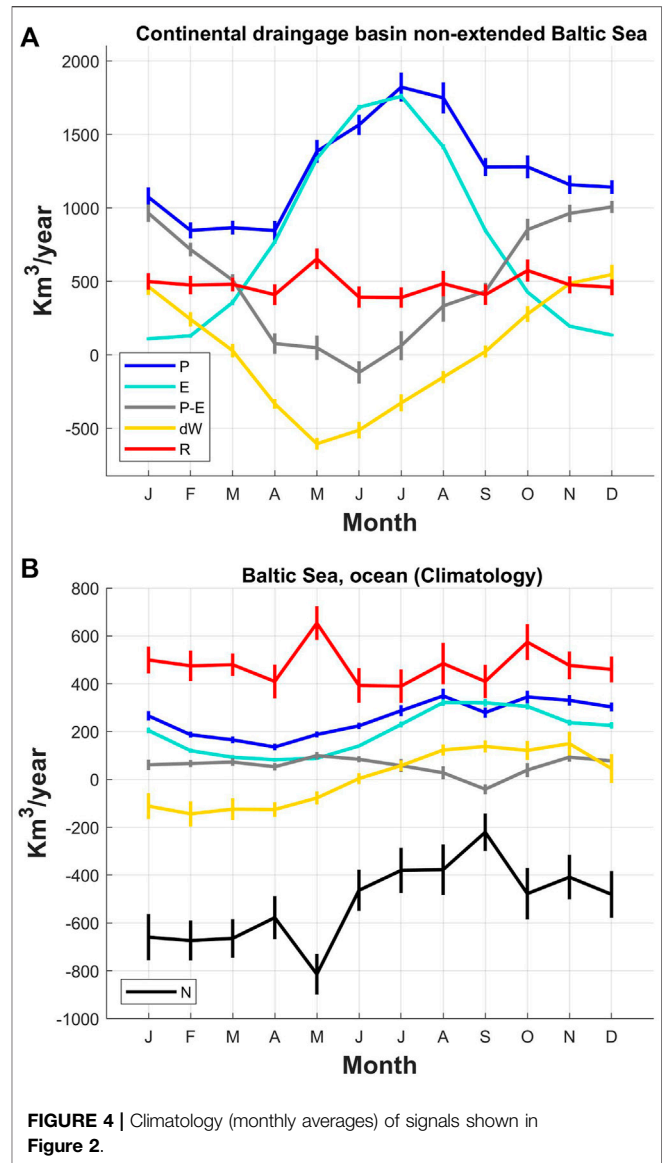


When the region is extended to include the Kattegat and Skagerrak straits, the drainage basin increases from  $1.64 \cdot 10^6 \text{ km}^2$  to  $2.01 \cdot 10^6 \text{ km}^2$ , and the oceanic surface area increases from  $0.38 \cdot 10^6 \text{ km}^2$  to  $0.45 \cdot 10^6 \text{ km}^2$ . On land, the net precipitation increases to  $P-E = 628 \pm 23 \text{ km}^3/\text{year}$ , and the drainage to the sea increases to  $R = 618 \pm 21 \text{ km}^3/\text{year}$  (Table 3). In the ocean, net precipitation is  $73 \pm 8 \text{ km}^3/\text{year}$ , which together with the contribution of  $R$  yields a net outflow to the North Sea of  $668 \pm 32 \text{ km}^3/\text{year}$ . A schematic representation of the averaged water cycle of the Baltic Sea and that of the extended Baltic Sea are shown in Figure 3.

### Seasonal Signal of WT

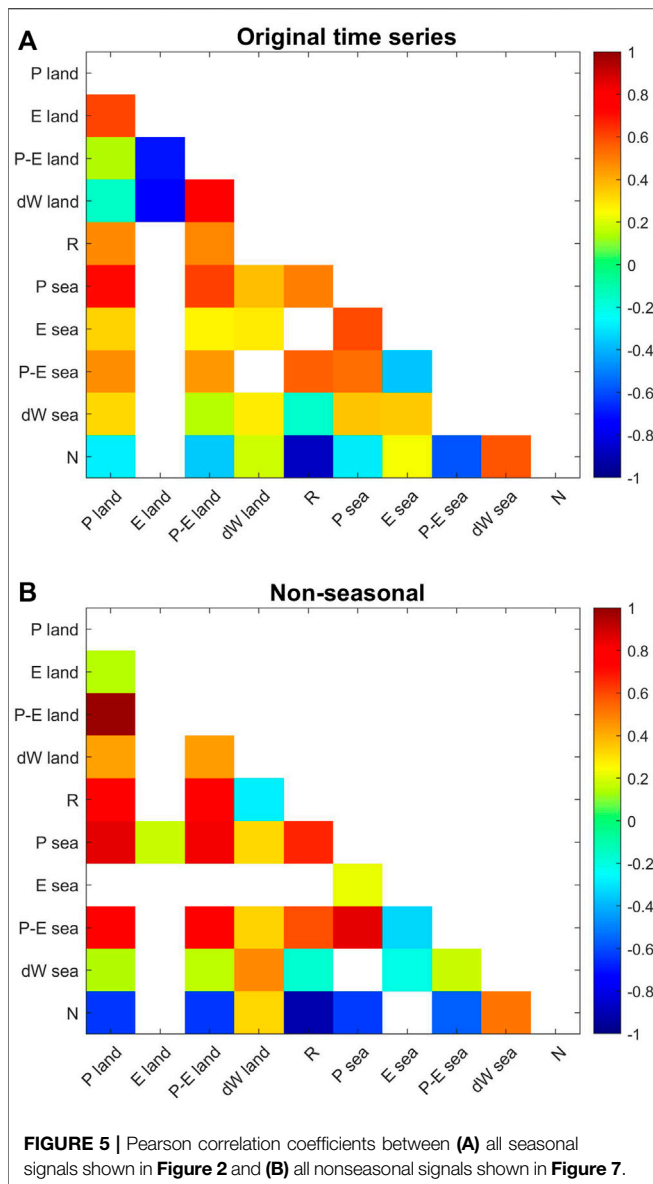
The Baltic Sea (either including the Kattegat and Skagerrak straits or not) receives an excess of fresh water that must leave the basin. However, the water mass imbalance is not compensated instantaneously, and a climatological signal arises in all WT components and water mass budgets. To analyze such climatology, the annual cycle of each WT component is estimated by averaging the signal of all Januarys, all Februarys, and so on. Figure 4 shows the average year or climatology for all WT components displayed in Figure 2.

In the continental drainage region of the Baltic Sea, both  $P$  and  $E$  climatologies show a good agreement in spring and summer, with maximum values of  $1,822 \pm 99 \text{ km}^3/\text{year}$  and  $1,759 \pm 18 \text{ km}^3/\text{year}$  occurring in July for  $P$  and  $E$ , respectively (Figure 4A). In autumn and winter,  $E$  is reduced much more than  $P$ , reaching a minimum of  $109 \pm 10 \text{ km}^3/\text{year}$  in December and January. This disagreement during the cold season is probably due to the increase of snow percentage in  $P$ , which is harder to evaporate than liquid water. This result agrees with the annual cycle of  $dW$ , which mimics the  $P-E$  climatology, showing a Pearson correlation of  $0.81 \pm 0.02$  between the original time series (Figure 5A). Positive (negative) values of  $dW$  represent an increase (decrease) in the water budget. In particular,  $dW$  shows a mean value of  $340 \pm 80 \text{ km}^3/\text{year}$  for autumn and winter, when snow accumulation (and low  $E$ ) is expected, and  $-317 \pm 95 \text{ km}^3/\text{year}$  for spring and summer, when ice melting (and  $E$ ) takes place.  $dW$  and  $E$  are strongly



anticorrelated, showing a correlation coefficient of  $-0.76 \pm 0.02$  between their original time series. The annual maximum and minimum of  $dW$  are reached in December ( $547 \pm 66 \text{ km}^3/\text{year}$ ) and May ( $-605 \pm 40 \text{ km}^3/\text{year}$ ), respectively. This minimum is produced by the annual maximum of  $R = 654 \pm 71 \text{ km}^3/\text{year}$ , although there is no significant correlation between  $dW$  and  $R$ .

In the Baltic Sea, the annual cycle of  $dW$  mimics that of  $P$  and  $E$ , despite Pearson correlations between the original time series being  $0.36 \pm 0.05$  and  $0.35 \pm 0.045$ , respectively. Hereafter, when SD is given with more than two decimals, it is used to reconstruct the 95% CI as plus/minus 2 SD if needed. Both  $dW$  and  $P$  present maximum values from August to November and minimum from February to April (Figure 4B). The annual maximum of  $E$  is reached between August and October, while the annual minimum takes place between February and May, when sea-ice coverage is maximum (Omstedt et al., 1997; Vihma and



Haapala, 2009). The larger values of  $dW$  found during the second half of the year represent an increase in the water budget, which is related to a minimum net outflow  $N = 390 \pm 42 \text{ km}^3/\text{year}$  from July to December. From January to May,  $N$  is almost doubled up to  $678 \pm 38 \text{ km}^3/\text{year}$ . Except for this half-year difference,  $N$  mirrors the month-to-month variability of  $R$ , presenting a significant Pearson correlation between the original time series of  $-0.88 \pm 0.015$  (Figure 6A), reminding that negative values of  $N$  represent the Baltic outflow. Then the greater the  $R$ , the larger (in absolute value) the  $N$ , that is, the larger the output. As shown in Figure 4B, the annual maximum of  $R$  ( $654 \pm 71 \text{ km}^3/\text{year}$ ) is reached in May, which results in the annual maximum magnitude of  $N$  ( $814 \pm 85 \text{ km}^3/\text{year}$ ).

The seasonal signals of WT components, of both continental and oceanic regions, in the extended Baltic Sea are almost identical to those of the (non-extended) Baltic Sea, although

with larger absolute values for  $P$ ,  $E$ ,  $R$ , and  $N$  (Supplementary Figure S2).

## Nonseasonal Signal of WT

The nonseasonal signal is obtained by subtracting the climatology from the original signal. This way is more appropriate than fitting an annual sinusoid since the average year is not always sinusoidal in shape (Figure 4). In general, all components show a larger nonseasonal variability on land than in the ocean (Figure 7). All components present a nonsignificant linear trend.

On land, the nonseasonal variability of  $P$  is the largest one, and it is propagated to  $P-E$ ,  $dW$ , and  $R$ . Pearson correlation coefficients between  $P$  and  $P-E$ ,  $R$ , and  $dW$  are  $0.98 \pm 0.0025$ ,  $0.74 \pm 0.035$ , and  $0.42 \pm 0.06$ , respectively (Figure 5B). Note that 1) the correlation between the original time series of  $P$  and  $P-E$  was very low ( $0.15 \pm 0.05$ ), but there is a high correlation of  $0.98 \pm 0.003$  between the nonseasonal time series; 2) the correlation between the original time series of  $P-E$  and  $E$  is  $-0.70 \pm 0.025$ , but it is not statistically significant between the nonseasonal time series. This means that  $P-E$  on land is driven by  $E$  at a seasonal scale and by  $P$  at a non-seasonal one. In the Baltic Sea,  $P$  and  $P-E$  show a high correlation ( $0.85 \pm 0.025$ ) for the nonseasonal signals and a lower one for the original signals ( $0.53 \pm 0.05$ ). On the contrary,  $E$  and  $P-E$  show a similar correlation around  $-0.35 \pm 0.065$  for both seasonal and nonseasonal signals. Then,  $P$  has more influence than  $E$  on  $P-E$  variability at both seasonal and nonseasonal scales. It is also significant that the  $P$  signal is similar over both continents and ocean (the corresponding correlation coefficient is  $0.86 \pm 0.025$ ), unlike  $E$ , for which no significant correlation is found between the continental and oceanic signals.

The interannual variability of  $P$ ,  $P-E$ , and  $R$  is quite strong, showing differences of around  $200\text{--}250 \text{ km}^3/\text{year}$  between some annual averages. Such differences even reach values around  $470 \text{ km}^3/\text{year}$  for  $N$ . For example, in 2012, both  $P$  and  $P-E$  showed an above-average annual mean value of  $1,406 \text{ km}^3/\text{year}$  and  $643 \text{ km}^3/\text{year}$ , respectively, which produced a maximum  $R = 658 \text{ km}^3/\text{year}$ . On the contrary, in 2006, a below-average  $P = 1,159 \text{ km}^3/\text{year}$  produced a below-average  $P-E = 444 \text{ km}^3/\text{year}$ , which in turn produced a below-average  $R = 395 \text{ km}^3/\text{year}$ . Although  $P-E$  was  $40 \text{ km}^3/\text{year}$  lower than average during this year,  $R$  decreased double that amount,  $81 \text{ km}^3/\text{year}$ , because there was an extra accumulation of water in the continents of  $41 \text{ km}^3/\text{year}$ . On the other hand, the correlation between  $R$  and  $N$  increases in magnitude from  $-0.88 \pm 0.015$  (original series in Figure 2) to  $-0.92 \pm 0.01$  for the nonseasonal signals (Figure 6). This means that the water transported by  $R$  into the Baltic Sea produces almost simultaneously, or with a lag of less than a month, an outflow from the Baltic Sea. The above-average  $R$  in 2012 produced an above-average outflow of water mass from the Baltic Sea of  $833 \text{ km}^3/\text{year}$ , while the below-average  $R$  in 2006 reduced  $N$  to more than half until  $360 \text{ km}^3/\text{year}$ . The reduction of  $N$  is larger than that of  $R$  because  $P-E$  over the Baltic Sea also showed an above-average annual mean in 2012 ( $110 \text{ km}^3/\text{year}$ ) and a below-average in 2006 ( $53 \text{ km}^3/\text{year}$ ) that increased and reduced  $N$ , respectively.

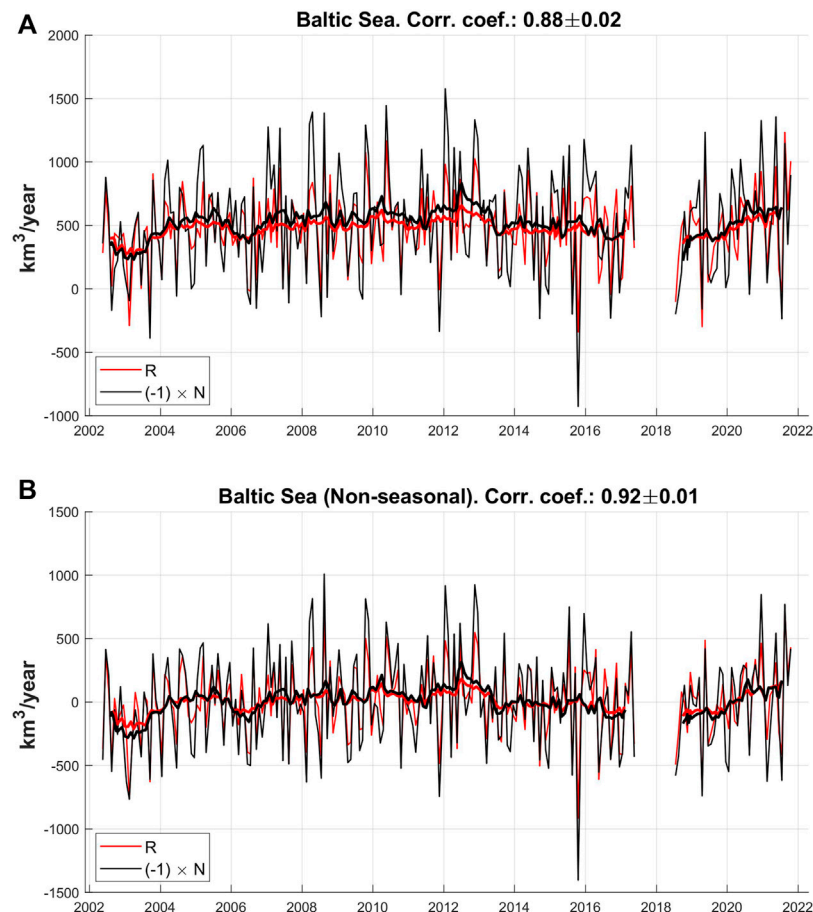


**FIGURE 6 | (A)** Seasonal and **(B)** nonseasonal water transport from land to the Baltic Sea (red curve) and net outflow from the Baltic Sea (black curve). Black curve represents  $-N$ . As  $N$  is multiplied by  $-1$ , positive (negative) values of black curve represent above-average (below-average) flows. Correlations between  $R$  and  $N$  are negative in both cases.

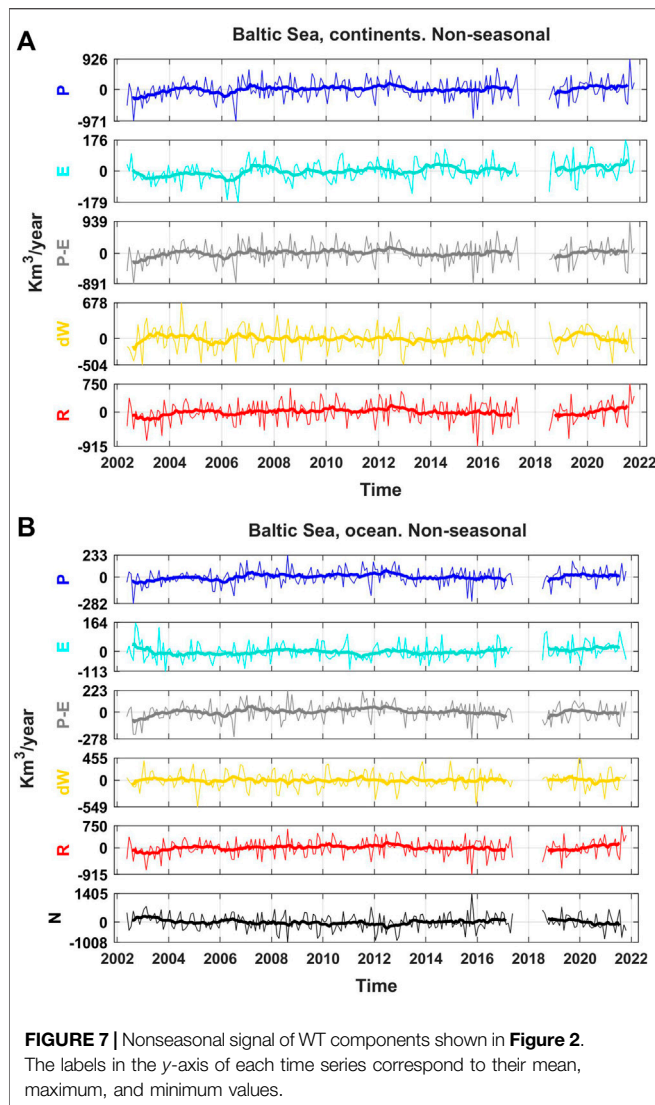
Although the climatology of  $N$  shows an outflow from the Baltic Sea every month of the year, it can sporadically reverse. For example, in October 2015, the net WT was  $N = 927 \text{ km}^3/\text{year}$  ( $1,400 \text{ km}^3/\text{year}$  more than the average value in October), which represented a huge net inflow to the Baltic Sea from the Atlantic Ocean that doubled the mean outflow of the 2002–2021 period. This event was produced by extremely low values of  $R$  and unusual high net evaporation over the Baltic Sea (Figures 6, 7), that is, by a decrease of freshwater input. On the other hand, a positive value of  $dW$  indicates an increment of the water mass budget in the Baltic Sea, which should have been produced by a Major Baltic Inflow (MBI). The MBI plays an important role in the Baltic Sea conditions because it introduces large volumes of saline and oxygen-rich water into the bottom layers that partially determine the faunal and floral composition. These three events (low  $R$ , high net  $E$ , and MBI) agree with the fact that the lower the runoff, the larger the deep-water salinity (Hänninen et al., 2000). However, note that  $N$  is not a direct estimate of MBI since some water transport models suggest that an increase in the outflow in the uppermost layer is related to an increase in the inflow in the bottom layer (Lehman and Hinrichsen, 2002).

Mohrholz et al. (2015) reported a very strong MBI produced by wind anomalies in December 2014. In that month,  $N$  showed  $523 \text{ km}^3/\text{year}$  more than the average value found for all Decembers, which is a third of the anomaly reported in October 2015. However, the MBI of December 2014 was stronger than that of October 2015 (Mohrholz, 2018).

The extended Baltic Sea shows the same kind of nonseasonal variability (Supplementary Figure S3) and the relationship between the WT components (Supplementary Figures S4, S5) above shown for the Baltic Sea.

### Influence of NAO on WT

The NAO is a climate atmospheric index that summarizes the surface pressure variability over the North Atlantic. It can be estimated as the sea level air pressure differences between the high-pressure system located over the Azores islands and the low-pressure system over Iceland. Then, changes in the NAO are associated with changes in the westerly winds in the North Atlantic, which influence weather conditions in Europe and eastern North America. In particular, NAO effects are stronger in winter, when positive (negative) phases of NAO produce above-average (below-average)  $P$  and temperature in northern



Europe, and below-average (above-average)  $P$  and temperature in the Mediterranean region and Hudson Bay area (Hurrell, 1995; Hurrell et al., 2003). In the Baltic Sea, positive (negative) winter NAO decreases (increases) the sea-ice extent (Omstedt and Chen, 2001; Heino et al., 2008), and rises (drops) the sea level (Andersson, 2002). We explore the influence of winter NAO on WT components of the Baltic Sea region as follows. The NAO index estimated by NOAA (<https://www.cpc.ncep.noaa.gov/products/precip/CWlink/pna/nao.shtml>; data accessed on 26/01/2022) and the nonseasonal time series shown in **Figure 7** are averaged over winter months (December to March), and their Pearson correlation coefficients are estimated. Only 5 out of the 10 WT components present a statistically significant correlation:  $0.64 \pm 0.09$  for continental  $P$ ,  $0.78 \pm 0.05$  for continental  $E$ ,  $0.52 \pm 0.12$  for continental  $P-E$ ,  $0.39 \pm 0.16$  for oceanic  $P$ , and  $0.55 \pm 0.12$  for oceanic  $P-E$ . We have not found a significant correlation between NAO and  $R$  for the period 2002–2021, but it does not mean that it does not exist for a different period. For example, Johansson (2016) found a correlation of 0.47 between NAO and

runoff for the period 1990–2009, but not for the period 1960–1979.

## DISCUSSION

Assuming the water budget equation, we used an atmospheric reanalysis and satellite-based time-variable gravity data to estimate the hydrological cycle of the Baltic Sea and its continental catchment region for the period 2002–2021. We provide the annual mean, climatology, and nonseasonal signals for all WT components. In general, the mean hydrological cycle and the climatology of  $P-E$  are similar to those reported by Jacob (2001) from a global and a regional climate model.

We have estimated a freshwater input from the continent, including superficial runoff (in river courses or not) and underground water discharge, of  $R = 476 \pm 17 \text{ km}^3/\text{year}$ . Our results about the climatology of  $R$  share some important features with previous studies based on almost a century of data and reconstructed data. In agreement with the existing literature (Cyberski and Wróblewski, 2000; Meier and Kauker, 2003), we found an annual maximum in May. There are, however, some important differences. In particular, in comparison with previous studies of the climatology of  $R$ , we found: 1) a lower annual range ( $264 \text{ km}^3/\text{year}$  versus  $\sim 480 \text{ km}^3/\text{year}$ ); 2) a larger increase from September to the local maxima in October ( $164 \text{ km}^3/\text{year}$  versus  $12 \text{ km}^3/\text{year}$ ); and 3) a lower annual maximum ( $654 \text{ km}^3/\text{year}$  versus  $728 \text{ km}^3/\text{year}$ ). These differences may be a consequence of a real change in the climatology but also of the different periods and methodology used. At the interannual scale, we have reported values of  $R = 395 \text{ km}^3/\text{year}$  in 2006 and  $R = 658 \text{ km}^3/\text{year}$  in 2012. This type of variability has been observed in previous studies. For example, Winsor et al. (2001) reported an annual mean river runoff of  $\sim 330 \text{ km}^3/\text{year}$  in 1976 and  $\sim 535 \text{ km}^3/\text{year}$  in 1981 (see also Meier and Kauker, 2003).

Another key result of this study is the estimated net water mass exchange between the Baltic Sea and the Atlantic Ocean. We report a mean net outflow of  $515 \pm 27 \text{ km}^3/\text{year}$  that evacuates the surplus of fresh water in the Baltic Sea, whose 92% comes from  $R$ . In addition,  $N$  shows a clear annual cycle with an amplitude of  $189 \pm 39 \text{ km}^3/\text{year}$  that peaks around September 16. On average, all months present a net outflow from the Baltic Sea, although in particular months,  $N$  flows in the opposite direction. On top of the climatology,  $N$  shows a significant interannual variability mainly driven by  $R$ . It is worth noting that such interannual variability is observed in both surface outflow and near-bottom inflow (Lehmann and Hinrichsen, 2002).

## CONCLUSION

During the last 2 decades, knowledge of the dynamics of the Earth system has undergone a tremendous advance, thanks to the GRACE missions, whose data have become key for many new applications aimed to enhance our knowledge in relevant problems. In this study, we illustrate the fundamental role of GRACE data for the study of the net seawater mass exchange in

the Baltic Sea (and the hydrological cycle in the region) using an algorithm proposed by García-García et al. (2020). When the exchange of water can only take place along one path, as is the case with semi-enclosed basins like the Baltic Sea, the algorithm provides net WT through that path. Using GRACE and ERA5 data as inputs, we have estimated the mean values, the climatology, and the interannual variability of the water exchange between the Baltic Sea and the open ocean, and also for an extended region including the Kattegat and Skagerrak straits. In this case, the mean net outflow from the extended Baltic Sea to the North Sea is  $668 \pm 32 \text{ km}^3/\text{year}$ , which is 30% larger than the net outflow from the non-extended Baltic Sea. This increment is produced by a continental contribution of  $618 \pm 21 \text{ km}^3/\text{year}$ , which is also an increase of 30% with respect to the non-extended Baltic Sea. In the annual amplitude, a smaller increment of 8% is observed, although it is not statistically significant. The overall conclusion is that the difference in water transport between the extended and non-extended regions considered in this study is mainly produced by the mean value.

The strengths of the methodology presented in this study are the following:

- 1) The results are independent of those reported in previous studies, which were mostly based on *in situ* observations and models.
- 2) The studied regions can be easily redefined, which makes possible the estimation of net water fluxes at any passage or section. This can be useful to make comparisons with independent studies or to define boundary conditions for oceanic models.
- 3) The results are based on two datasets (GRACE/GRACE-FO and ERA5) which are expected to be updated periodically. Therefore, the proposed methodology is a potential tool for continuously monitoring the hydrological cycle of the Baltic Sea, as well as to understand its time evolution. In this respect, when longer time series will be available, the proposed methodology would allow to detect the predicted changes consequence of the ongoing climate change.

## DATA AVAILABILITY STATEMENT

Publicly available datasets were analyzed in this study. These data can be found at: <https://cds.climate.copernicus.eu/cdsapp#!/>

## REFERENCES

- Andersson, H. C. (2002). Influence of Long-Term Regional and Large-Scale Atmospheric Circulation on the Baltic Sea Level. *Tellus A: Dynamic Meteorology Oceanography* 54 (1), 76–88. doi:10.3402/tellusa.v54i1.12125
- Bergström, S., and Carlsson, B. (1994). River Runoff to the Baltic Sea: 1950–1990. *Ambio. R. Swedish Acad. Sci.* 23 (4/5), 280–287.
- Chao, B. F. (2016). Caveats on the Equivalent Water Thickness and Surface Mascon Solutions Derived from the GRACE Satellite-Observed Time-Varyable Gravity. *J. Geod* 90, 807–813. doi:10.1007/s00190-016-0912-y

home <http://www2.csr.utexas.edu/grace> <https://www.cpc.ncep.noaa.gov/products/precip/CWlink/pna/nao.shtml>.

## AUTHOR CONTRIBUTIONS

DG-G designed the study. AB processed datasets and wrote the first draft of the manuscript. MT and MV implemented the bootstrap and contributed to other aspects of the data analysis. MV also provided funding for the research. All authors discussed and interpreted the results and contributed to the writing and revision of the manuscript.

## FUNDING

DG-G, MV, and MT are partially funded by the Spanish Ministry of Science, Innovation, and Universities grant number RTI2018-093874-B-100, and the Generalitat Valenciana grant number GVA-THINKINAZUL/2021/035. DG-G and MV are partially funded by the Generalitat Valenciana grant number PROMETEO/2021/030. J-MS thanks the joint funding received from Generalitat Valenciana and the European Social Fund under Grant APOSTD/2020/254. AB benefits from a doctoral study allowance financed by the Algerian Ministry of Higher Education and Scientific Research.

## ACKNOWLEDGMENTS

All data used in this study are publicly available, and we thank all the organizations that provided them: ERA5 data provided by the Copernicus Climate Change Service Climate Data Store (CDS), <https://cds.climate.copernicus.eu/cdsapp#!/home>; GRACE time-variable gravity data provided by CSR, University of Texas, <http://www2.csr.utexas.edu/grace>; and North Atlantic Oscillation (NAO) from NOAA Climate Prediction Center (CPC).

## SUPPLEMENTARY MATERIAL

The Supplementary Material for this article can be found online at: <https://www.frontiersin.org/articles/10.3389/feart.2022.879148/full#supplementary-material>

- Chao, B. F. (2005). On Inversion for Mass Distribution from Global (Time-variable) Gravity Field. *J. Geodynamics* 39, 223–230. doi:10.1016/j.jog.2004.11.001
- Chen, J., Tapley, B., Seo, K. W., Wilson, C., and Ries, J. (2019). Improved Quantification of Global Mean Ocean Mass Change Using GRACE Satellite Gravimetry Measurements. *Geophys. Res. Lett.* 46, 13984–13991. doi:10.1029/2019GL085519
- Cyberski, J., and Wróblewski, A. (2000). Riverine Water Inflows and the Baltic Sea Water Volume 1901–1990. *Hydrol. Earth Syst. Sci.* 4, 1–11. doi:10.5194/hess-4-1-2000
- Dargahi, B., and Cvetkovic, V. (2017). Tracer Transport and Exchange Processes in the Baltic Sea 2000–2009. *J. Oceanogr. Mar. Res.* 5, 156. doi:10.4172/2572-3103.1000156

- Dargahi, B., Kolluru, V., and Cvetkovic, V. (2017). Multi-layered Stratification in the Baltic Sea: Insight from a Modeling Study with Reference to Environmental Conditions. *Jmse* 5, 1–2. doi:10.3390/jmse5010002
- Durack, P. J., Wijffels, S. E., and Matear, R. J. (2012). Ocean Salinities Reveal Strong Global Water Cycle Intensification during 1950 to 2000. *Science* 336, 6080455–6080458. doi:10.1126/science.1212222
- Ellmann, A. (2004). Effect of the GRACE Satellite mission on Gravity Field Studies in Fennoscandia and the Baltic Sea Region. *Proc. Estonian Acad. Sci. Geology* 53 (2), 67–93. doi:10.3176/geol.2004.2.01
- Eom, J., Seo, K.-W., and Ryu, D. (2017). Estimation of Amazon River Discharge Based on EOF Analysis of GRACE Gravity Data. *Remote Sensing Environ.* 191, 55–66. doi:10.1016/j.rse.2017.01.011
- Fatolazadeh, F., and Goita, K. (2021). Mapping Terrestrial Water Storage Changes in Canada Using GRACE and GRACE-FO. *Sci. Total Environ.* 779, 146435. doi:10.1016/j.scitotenv.2021.146435
- García-García, D., Vigo, M.I., Trovati, M., Vargas, J., and Sayol, J.M. (2022). Hydrological cycle of the Mediterranean-Black Sea system. *Climate Dynamics*, 1–20. doi:10.1007/s00382-022-06188-2
- García-García, D., Vigo, M.I., and Trovati, M. (2020). Water transport among the world's ocean basins within the water cycle. *Earth Syst. Dynam.* 11, 1089–1106. doi:10.5194/esd-11-1089-2020
- Giorgi, F. (2006). Climate change hot-spots. *Geophys. Res. Lett.* 33, 8. doi:10.1029/2006GL025734
- Greve, P., Orłowsky, B., Mueller, B., Sheffield, J., Reichstein, M., and Seneviratne, S. I. (2014). Global Assessment of Trends in Wetting and Drying over Land. *Nat. Geosci* 7, 716–721. doi:10.1038/ngeo2247
- Gustafsson, B. (1997). Interaction between the Baltic Sea and the North Sea. *Deutsche Hydrographische Z.* 49, 165–183. doi:10.1007/bf02764031
- Häkanson, L., and Lindgren, D. (2010). Water Transport and Water Retention in Five Connected Subbasins in the Baltic Sea-Simulations Using a General Mass-Balance Modeling Approach for Salt and Substances. *J. Coastal Res.* 262 (2), 241–264. doi:10.2112/08-1082.1
- Hänninen, J., Mäkinen, K., Rajasilta, M., and Vuorinen, I. (2021). The Baltic Sea and the Adjacent North Sea Silicate Concentrations. *Estuarine, Coastal Shelf Sci.* 249, 107110. doi:10.1016/j.eccs.2020.107110
- Hänninen, J., Vuorinen, I., and Hjelt, P. (2000). Climatic Factors in the Atlantic Control the Oceanographic and Ecological Changes in the Baltic Sea. *Limnol. Oceanogr.* 45 (3), 703–710. doi:10.4319/lo.2000.45.3.0703
- Hänninen, J., and Vuorinen, I. (2011). Time-Varying Parameter Analysis of the Baltic Sea Freshwater Runoffs. *Environ. Model. Assess.* 16 (1), 53–60. doi:10.1007/s10666-010-9231-5
- Hansson, D., Eriksson, C., Omstedt, A., and Chen, D. (2011). Reconstruction of River Runoff to the Baltic Sea, AD 1500–1995. *Int. J. Climatol.* 31 (5), 696–703. doi:10.1002/joc.2097
- Hartmann, D. L. (1994). *Global Physical Climatology*. Amsterdam, the Netherlands: Elsevier.
- Heino, R., Tuomenvirta, H., Vuglinsky, V. S., and Gustafsson, B. G. (2008). “Past and Current Climate Change,” in *The BACC Author Team Assessment of Climate Change for the Baltic Sea Basin* (Berlin-Heidelberg: Springer-Verlag), 72. doi:10.1007/978-3-540-72786-6\_2
- Held, I. M., and Soden, B. J. (2006). Robust Responses of the Hydrological Cycle to Global Warming. *J. Clim.* 19 (21), 5686–5699. doi:10.1175/jcli3990.1
- Hersbach, H., de Rosnay, P., Bell, B., Schepers, D., Simmons, A., Soci, C., et al. (2018). *Operational Global Re-Analysis: Progress, Future Directions, and Synergies with NWP. ERA Report Series 27*. Shinfield Park, Reading, Berkshire, England: European Centre for Medium Range Weather Forecasts.
- Huntington, T. G. (2006). Evidence for Intensification of the Global Water Cycle: Review and Synthesis. *J. Hydrol.* 319 (1–4), 83–95. doi:10.1016/j.jhydrol.2005.07.003
- Hurrell, J. W. (1995). Decadal Trends in the North Atlantic Oscillation: Regional Temperatures and Precipitation. *Science* 269 (5224), 676–679. doi:10.1126/science.269.5224.676
- Hurrell, J. W., Kushnir, Y., Ottersen, G., and Visbeck, M. (2003). *An Overview of the North Atlantic Oscillation*. Washington: Washington American Geophysical Union Vol. 134, 1–35. doi:10.1029/134GM01
- Jacob, D. (2001). A Note to the Simulation of the Annual and Inter-annual Variability of the Water Budget over the Baltic Sea Drainage basin. *Meteorology Atmos. Phys.* 77 (1), 61–73. doi:10.1007/s007030170017
- Jin, S., and Feng, G. (2013). Large-scale Variations of Global Groundwater from Satellite Gravimetry and Hydrological Models, 2002–2012. *Glob. Planet. Change* 106, 20–30. doi:10.1016/j.gloplacha.2013.02.008
- Johansson, J. (2016). Total and Regional Runoff to the Baltic Sea. Baltic Sea Environment Fact Sheet. Available at: <http://www.helcom.fi/baltic-sea-trends/environment-fact-sheets/> (Accessed February 2022).
- Jordà, G., Von Schuckmann, K., Josey, S. A., Caniaux, G., García-Lafuente, J., Sammartino, S., et al. (2017). The Mediterranean Sea Heat and Mass Budgets: Estimates, Uncertainties and Perspectives. *Prog. Oceanogr.* 156, 174–208. doi:10.1016/j.pocean.2017.07.001
- Lee, E., Livino, A., Han, S.-C., Zhang, K., Briscoe, J., Kelman, J., et al. (2018). Land Cover Change Explains the Increasing Discharge of the Paraná River. *Reg. Environ. Change* 18 (6), 1871–1881. doi:10.1007/s10113-018-1321-y
- Lehmann, A., and Hinrichsen, H. H. (2002). Water, Heat, and Salt Exchange between the Deep Basins of the Baltic Sea. *Boreal Environ. Res.* 7 (4), 405–415.
- Li, Q., Zhong, B., Luo, Z., and Yao, C. (2016). GRACE-based Estimates of Water Discharge over the Yellow River basin. *Geodesy. Geodynamics* 7 (3), 187–193. doi:10.1016/j.geog.2016.04.007
- Lorenz, C., Kunstmann, H., Devaraju, B., Tourian, M. J., Sneeuw, N., and Riegger, J. (2014). Large-Scale Runoff from Landmasses: A Global Assessment of the Closure of the Hydrological and Atmospheric Water Balances\*. *J. Hydrometeorology* 15 (6), 2111–2139. doi:10.1175/JHM-D-13-0157.s1
- Markonis, Y., Papalexiou, S. M., Martinkova, M., and Hanel, M. (2019). Assessment of Water Cycle Intensification over Land Using a Multisource Global Gridded Precipitation Dataset. *J. Geophys. Res. Atmos.* 124 (21), 11175–11187. doi:10.1029/2019JD030855
- Matthäus, W., and Schinke, H. (1999). The Influence of River Runoff on Deep Water Conditions of the Baltic Sea. *Hydrobiologia. Biological, Phys. Geochemical Features Enclosed Semi-enclosed Mar. Syst.* 393, 1–10.
- Meier, H. E. M., and Döschner, R. (2002). Simulated Water and Heat Cycles of the Baltic Sea Using a 3D Coupled Atmosphere – Ice – Ocean Model. *Boreal Environ. Res.* 7, 327–334.
- Meier, H. E. M., and Kauker, F. (2003). Modeling Decadal Variability of the Baltic Sea: 2. Role of Freshwater Inflow and Large-Scale Atmospheric Circulation for Salinity. *J. Geophys.* 108, 1–10. doi:10.1029/2003jco01799
- Mikulski, Z. (1986). Water balance of the Baltic Sea. *Geophysica* 17120 (1–2), 159.
- Mohrholz, V. (2018). Major Baltic inflow statistics - Revised. *Front. Mar. Sci.* 5. doi:10.3389/fmars.2018.00384
- Mohrholz, V., Naumann, M., Nausch, G., Krüger, S., and Gräwe, U. (2015). Fresh oxygen for the Baltic Sea - an exceptional saline inflow after a decade of stagnation. *J. Marine Sys.* 148, 152–166. doi:10.1016/j.jmarsys.2015.03.005
- Oki, T., and Sud, Y. C. (1998). Design of Total Runoff Integrating Pathways (TRIP)-A Global River Channel Network. *Earth Interact.* 2, 1–37. doi:10.1175/1087-3562(1998)002<0001:dotrip>2.3.co;2
- Omstedt, A., and Chen, D. (2001). Influence of atmospheric circulation on the maximum ice extent in the Baltic Sea. *J. Geophys. Res.* 106, 4493–4500. doi:10.1029/1999jc000173
- Omstedt, A., Elken, J., Lehmann, A., and Piechura, J. (2004). Knowledge of the Baltic Sea physics gained during the BALTEX and related programs. *Progress Oceanography* 63, 1–28. doi:10.1016/j.pocean.2004.09.001
- Omstedt, A., Meuller, L., and Nyberg, L. (1997). Interannual, seasonal, and regional variations of precipitation and evaporation over the Baltic Sea. *Ambio* 26 (8), 484–492.
- Omstedt, A., and Nohr, C. (2004). Calculating the water and heat balances of the Baltic Sea using ocean modeling and available meteorological, hydrological, and ocean data. *Tellus A: Dynamic Meteorology and Oceanography* 56 (4), 400–414. doi:10.3402/tellusa.v56i4.14428
- Omstedt, A., and Rutgersson, A. (2000). Closing the Water and Heat Cycles of the Baltic Sea. *metz* 9 (1), 59–66. doi:10.1127/metz/9/2000/59
- Pajak, K., and Birylo, M. (2017). Seasonal Baltic Sea Level Changes in Coastal Zone. *Eur. Water* 59, 185–192.
- Patton, A., Politis, D. N., and White, H. (2009). Correction to “Automatic Block-Length Selection for the Dependent Bootstrap”. *Economet. Rev.* 28, 372–375. doi:10.1080/07474930802459016
- Peltier, W. R., Argus, D. F., and Drummond, R. (2018). Comment on “An Assessment of the ICE-6GC (VM5a) Glacial Isostatic Adjustment Model” by Purcell et al. *J. Geophys. Res.-Solid* 123, 2019–2028. doi:10.1002/2016JB013844

- Placke, M., Meier, H. E. M., Gräwe, U., Neumann, T., Frauen, C., and Liu, Y. (2018). Long-term Mean Circulation of the Baltic Sea as Represented by Various Ocean Circulation Models. *Front. Mar. Sci.* 5, 287. doi:10.3389/fmars.2018.00287
- Politis, D. N., and Romano, J. P. (1994). The Stationary Bootstrap. *J. Am. Stat. Assoc.* 89, 1303–1313. doi:10.1080/01621459.1994.10476870
- Save, H. (2019). CSR GRACE RL06 Mascon Solutions, Texas Data Repository Dataverse. doi:10.18738/T8/UN91VR
- Save, H., Bettadpur, S., and Tapley, B. D. (2016). High Resolution CSR GRACE RL05 Mascons. *J. Geophys. Res.-Solid* 121, 7547–7569. doi:10.1002/2016JB013007
- Stramska, M., and Aniskiewicz, P. (2019). Satellite Remote Sensing Signatures of the Major Baltic Inflows. *Remote Sensing* 11, 954. doi:10.3390/rs11080954
- Sun, Y., Riva, R., and Ditmar, P. (2016). Optimizing Estimates of Annual Variations and Trends in Geocenter Motion and J2 From a Combination of GRACE Data and Geophysical Models. *J. Geophys. Res. Solid Earth* 121. doi:10.1002/2016JB013073
- Swenson, S., Chambers, D., and Wahr, J. (2008). Estimating Geo- Center Variations From a Combination of GRACE and Ocean Model Output. *J. Geophys. Res.* 113, B08410. doi:10.1029/2007JB005338
- Syed, T. H., Famiglietti, J. S., and Chambers, D. P. (2009). GRACE-based Estimates of Terrestrial Freshwater Discharge from basin to continental Scales. *J. Hydrometeorology* 10 (1), 22–40. doi:10.1175/2008JHM993.1
- Syed, T. H., Famiglietti, J. S., Chen, J., Rodell, M., Seneviratne, S. I., Viterbo, P., et al. (2005). Total basin Discharge for the Amazon and Mississippi River Basins from GRACE and a Land-Atmosphere Water Balance. *Geophys. Res. Lett.* 32 (24), 1–5. doi:10.1029/2005GL024851
- The BACC Author Team (2008). *Assessment of Climate Change for the Baltic Sea basin*. Berlin: Springer Science & Business Media. doi:10.1007/978-3-540-72786-6
- Vihma, T., and Haapala, J. (2009). Assessment of Climate Change for the Baltic Sea Basin. *Prog. Oceanography* 80 (3–4), 129–148. doi:10.1016/j.pocean.2009.02.002
- Virtanen, J., Mäkinen, J., Bilker-Koivula, M., Virtanen, H., Nordman, M., Kangas, A., et al. (2010). Baltic Sea Mass Variations from GRACE: Comparison with *In Situ* and Modelled Sea Level Heights. *Gravity. Geoid. Earth Observation* 135, 571–577. doi:10.1007/978-3-642-10634-7\_76
- Wahr, J., Molenaar, M., and Bryan, F. (1998). Time Variability of the Earth's Gravity Field: Hydrological and Oceanic Effects and Their Possible Detection Using GRACE. *J. Geophys. Res.* 103 (30), 229. doi:10.1029/98jb02844
- Winsor, P., Rodhe, J., and Omstedt, A. (2001). The Baltic Sea Ocean Climate: an Analysis of 100 Yr of Hydrographic Data with Focus on the Freshwater Budget. *Clim. Res.* 18 (1–2), 5–15. doi:10.3354/cr018005
- Wouters, B., Bonin, J. A., Chambers, D. P., Riva, R. E. M., Sasgen, I., and Wahr, J. (2014). GRACE, Time-Varying Gravity, Earth System Dynamics and Climate Change. *Rep. Prog. Phys.* 77, 116801. doi:10.1088/0034-4885/77/11/116801

**Conflict of Interest:** The authors declare that the research was conducted in the absence of any commercial or financial relationships that could be construed as a potential conflict of interest.

**Publisher's Note:** All claims expressed in this article are solely those of the authors and do not necessarily represent those of their affiliated organizations, or those of the publisher, the editors, and the reviewers. Any product that may be evaluated in this article, or claim that may be made by its manufacturer, is not guaranteed or endorsed by the publisher.

Copyright © 2022 Boulahia, García-García, Vigo, Trottini and Sayol. This is an open-access article distributed under the terms of the Creative Commons Attribution License (CC BY). The use, distribution or reproduction in other forums is permitted, provided the original author(s) and the copyright owner(s) are credited and that the original publication in this journal is cited, in accordance with accepted academic practice. No use, distribution or reproduction is permitted which does not comply with these terms.